Triangular flow induced hyperon polarization

Summer student report

Janiely Ribeiro Barbosa

Supervisors: Sourav Kundu, Junlee Kim

October 1, 2024

Abstract

In relativistic high-energy collisions, the resulting system often behaves almost like a perfect fluid. Particularly in peripheral collisions, the interacting area forms an elliptical geometry, creating a pressure gradient that leads to momentum anisotropy in particle production. Furthermore, this momentum anisotropy creates local vortices which are directed along the beam direction and leads to a polarization of produced hadron with non-zero spin. Experimentally, the polarization originating from anisotropic expansion can be studied by measuring lambda polarization by utilizing its property of parity-violating decay In Run 2, ALICE Collaboration has already measured the Λ hyperon polarization as a function of the azimuthal angle relative to the the second order event plane with respect to the beam axis. In this project, using the high statistics Run 3 Pb–Pb collisions, we extended these measurements as a function of the azimuthal angle relative to the third order event plane to probe the triangular flow induced hyperon polarization.

Acknowledgments

I want to express my gratitude to my supervisors, Sourav Kundu and Junlee Kim, thank you for dedicating your time to teaching and supporting me. Also I thank the ALICE group for warmly welcoming me. I am grateful to CERN for the opportunity to be a summer student for 2 months, it was truly a once-in-a-lifetime experience.

Contents

1 Introduction

The fluid properties of the system formed in heavy-ion collisions are of great interest to many studies. Its properties such as shear and bulk viscosity are sensitive to the mommentum distribution of produced particle. Therefore, it is essential to study and quantify these effects to fully understand the nature of the system and its influence on the outcomes.

This project focuses on the lambda hyperon polarization resulted from early dynamics of heavy-ion collisions, particularly examining how the initial shape of the collision correlates with higher-order flow harmonics. The lambda hyperon is chosen due to its parity-violating decay, which causes the emitted proton daughter particle to be preferentially aligned with the Λ's spin direction. By tracking the momentum of the emitted proton daughter, it is possible to directly correlate it with the original lambda spin and, consequently, determine its polarization.

2 Induced Polarization

In non-central heavy-ion collisions, such as Pb-Pb, the initial collision geometry is approximately elliptical (see Fig. 9a). This shape creates a pressure gradient that results in a preferential emission of particles along the shorter axis, leading to a velocity gradient. The velocity gradient originated in the transverse plane is sensitive to the shear and bulk viscosity of the medium. This velocity gradient forms vorticity in the transverse plane of the medium which is directed along or opposite to the beam direction (Z direction in Fig. 1) depending upon the azimuthal angle of particle emission. Due to the azimuthal dependence of produced vorticity, polarization originating from the anisotropic expansion has a quadrupole structure in the azimuthal angle of particle emission.

The ALICE experiment during Run 2 successfully measured and reported on the polarization of lambda hyperons. The objective here is to extend this analysis to include the third-order triangular flow (see Fig. 1b) using the high-statistics data from Run 3.

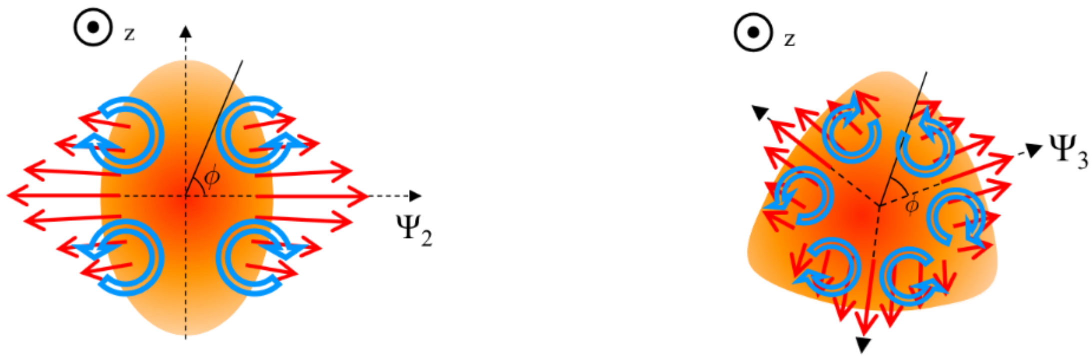

(a) (b)

Figure 1: Initial shape for elliptical and triangular flow respectively, the red arrows indicate the pressure gradient while the blue twirls indicate the vorticity which changes for each of the event planes [1].

The geometry of the problem is defined with the beam direction aligned along the Z-axis and the event plane lying in the XY plane. As illustrated in Fig. 1, the polarization along the Z-axis varies depending on the section of the event plane, giving it a sinusoidal pattern. This can be expressed through a Fourier decomposition:

$$P_{z,sn} = \frac{\left\langle 1 + 2P_z \sin(n\phi - n\Psi_n^{EP}) \right\rangle}{R} \tag{1}$$

In Eq. 1, the suffix $n = \{2, 3\}$ represents the nth order of the event plane. Here, ϕ is the azimuthal angle between the emitted particle's momentum and the event plane, and Ψ denotes the flow plane angle and R the event plane resolution.

In the ALICE experiment data, measurements were taken for Pb-Pb collisions at $\sqrt{S_{NN}} = 5.36\,\text{TeV}$. The Λ and $\bar{\Lambda}$ hyperons were reconstructed using the V0 reconstruction technique mentioned earlier.

The relation for the measured polarization along the z-axis, relative to the event plane, is given by Equation 2. In this equation, $P_{z,sn}$ denotes the measured polarization, φ is the azimuthal emission angle of the particle, Ψ_n^{EP} is the event plane angle, and $R(\Psi_n^{EP})$ is the event plane resolution. The index $n = \{2, 3\}$ refers to the order of the event plane.

$$P_{z,sn} = \frac{\left\langle P_z \sin(n\varphi - n\Psi_n^{EP}) \right\rangle}{R(\Psi_n^{EP})} \tag{2}$$

The polarization in the z-axis direction can be estimated using the following expression:

$$P_z(p_T, y_H, \varphi) = \frac{\left\langle \cos\theta_p^* \right\rangle}{\alpha_H \left\langle (\cos\theta_p^*)^2 \right\rangle}, \tag{3}$$

where α_H is the hyperon decay parameter, θ_p^* is the angle between proton in Lambda rest frame with the beam direction and $\left\langle (\cos\theta_p^*)^2 \right\rangle$ represents the finite detector acceptance, which has a value of 1/3 for an ideal detector.

3 Λ hyperon reconstruction in experiments

In real experiments, it is not possible to pinpoint Lambda particles as accurately as in event generator simulations like Pythia. Instead, to effectively identify events corresponding to the decay of a Lambda hyperon particle, V0 reconstruction is performed. The lambda hyperon decays in to two charged particles:

$$\Lambda \rightarrow \pi^- + p$$

Since most protons and pions are produced either on the global vertix or thermally through the decay of other particles is necessary to apply the reconstruction of the decay tracks and apply a series of topological cut criteria to ensure that both particles decayed from the same lambda and not from other background processes.

Following Fig.2 as referece, some of the conditions applied are:

- Minimum distance between the primary and secondary vertices: Due to the relatively long lifetime of the hyperon, it can travel some distance before decaying. Setting a minimum distance helps ensure that the decay particles did not originate from the global primary vertex.
- Minimum distance of the daughter tracks to the primary vertex: This criterion helps confirm that the decay products were not produced at the primary vertex, reducing contamination from non-signal particles.
- Distance of closest approach (DCA) for daughter tracks: A minimum DCA between the decay tracks is required to indicate that the daughter particles originated from the same decay vertex, rather than from two unrelated processes.
- Minimum opening angle of the daughter tracks: The decay products are expected to emerge with a certain opening angle due to the conservation of momentum. A minimum opening angle ensures that the particles are indeed decay products from the Lambda hyperon.

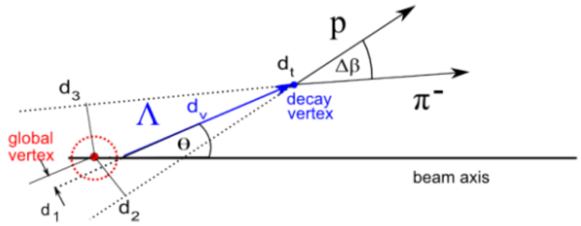

Figure 2: Topology of Λ decay [3]

Through the reconstruction of the tracks of the daughter particles is also possible to compute the invariant mass of the original lambda and theferore it's momentum.

4 MC pythia simulation

The initial step was to check for signs of polarization in the Pythia 3.8 event generator. To do this, a dataset from a simulation of 1000 inelastic collision events was analyzed, with a center-of-mass energy of $e_{CM} = 13000$ GeV and a transverse momentum range of $1.0 < p_T < 3.0$ GeV/c. The procedure involved selecting the Lambda particles using their PDG code and then identifying events where the daughter particles were a proton and a pion, considering only the absolute values to capture both Lambda and anti-Lambda decays.

After identifying the Lambda particles, a Lorentz boost was applied to the proton using the Lambda's momentum, allowing the measurements to be taken in the Lambda rest frame. The average of the angle θ_p^* was then recorded as a function of the transverse momentum p_T. The results of this analysis are presented in Fig.3.

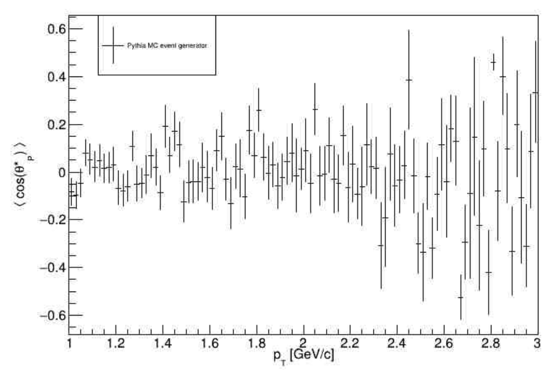

Figure 3: Average of cosine of θ_P^* in function of p_T for inellastic collision event generator in Pythia.

Fig.3 shows that the average cosine fluctuates around zero, indicating no evidence of polarization. This occurs because Pythia does not account for the flow that generates the polarization, resulting in outcomes that are consistently zero.

5 Data analysis

The quantity $Q = \left\langle \cos\theta_p^* \sin(n\varphi - 2\Psi_n^{EP}) \right\rangle$ is estimated for each of the invariant mass bin of Lambda, the polarization $P_{z,sn}$ can be estimated through a fit in the form of Equation 4:

$$Q(M_{inv}) = f^S(M_{inv})Q^S + f^{BG}Q^{BG}(M_{inv}), \tag{4}$$

where f^S represents the signal fraction, f^{BG} represents the background fraction $(1 - f^S)$, Q^S estimates the polarization signal, and Q^{BG} accounts for possible background interference. The polarization value is then obtained from the signal Q^S, corrected using the event plane resolution (see section 5.1), the decay parameter valued $\alpha_\Lambda = 0.750$, $\alpha_{\bar{\Lambda}} = -0.758$ and the finite detector acceptance.

5.1 Event Plane Resolution

The reaction plane is defined by the impact parameter (the distance between the centers of the two colliding nuclei) and the beam direction, with the angle Ψ_n is the angle between the event plane vector and the "x" axis. In experiments, the reaction plane cannot be measured directly, so the event plane, estimated from the azimuthal angle of the produced charged particles, is used as a proxy.

The event plane resolution is a measure of how well the event plane correlates with the actual reaction plane. A resolution value of 1 means the event plane is perfectly aligned with the reaction plane, while a value of 0.7 indicates a 70% probability that the event plane matches the reaction plane. The resolution varies with centrality due to its dependence on the impact parameter. The function used for its calculation in this study is shown in Fig.4 for both second and third-order event planes.

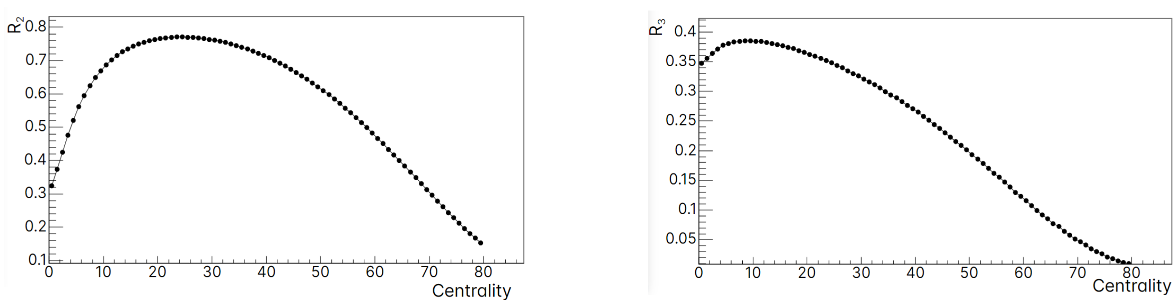

(a) (b)

Figure 4: Event plane resolution as a function of centrality for the ALICE Pb-Pb collision dataset at $\sqrt{S_{NN}} = 5.36$TeV

5.2 Second Order Event Plane

To apply the invariant mass method, the first step is to extract the signal distribution from the invariant mass spectrum. This is achieved by fitting the data with a function that combines a third-order polynomial to model the background and a Gaussian to represent the signal. Once the fitting is complete, the parameters of the Gaussian distribution are extracted, which then defines the final signal distribution. An example resulting graph of the signal plus background fitting of the invariant mass and the signal fraction can be found in Fig.5. The first analysis method involves fitting the average cosine profile as a function of the invariant mass, incorporating both the signal fraction and background as described in Eq.4. The parameter associated with the signal fraction corresponds to the polarization value. The profile and its fit are shown in Fig.6 for both Λ and $\bar{\Lambda}$, the results obtained were $P_{z,s2} = 0.00157 \pm 0.00037$ for Λ and $P_{z,s2} = 0.00219 \pm 0.00039$ for $\bar{\Lambda}$, which is compatible with the results obtained from ALICE in [2].

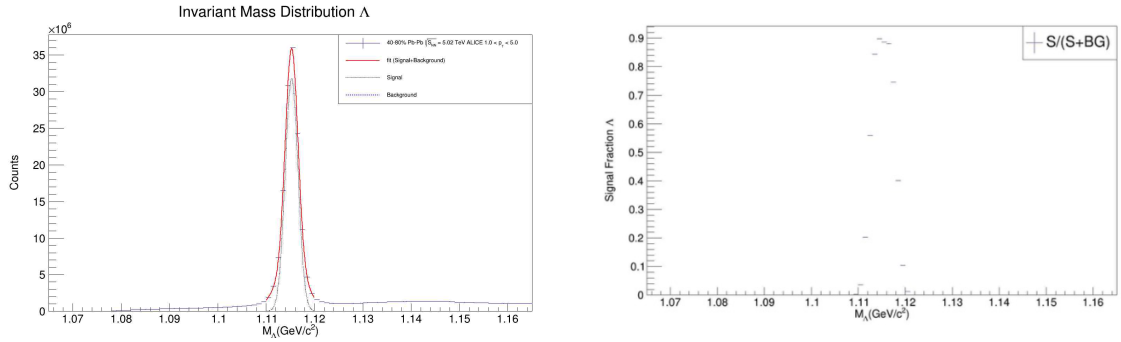

(a) (b)

Figure 5: **(a)** Invariant mass distribution for the Λ hyperon in the ALICE Pb-Pb $\sqrt{S_{NN}} = 5.36$ TeV dataset, within 40-80% centrality and a transverse momentum range of $1.0 < p_T < 5.0$ GeV/c. The red line represents the fit combining signal and background, the black dotted line shows the signal component, and the blue dotted line indicates the background. **(b)** Signal fraction derived from the fit.

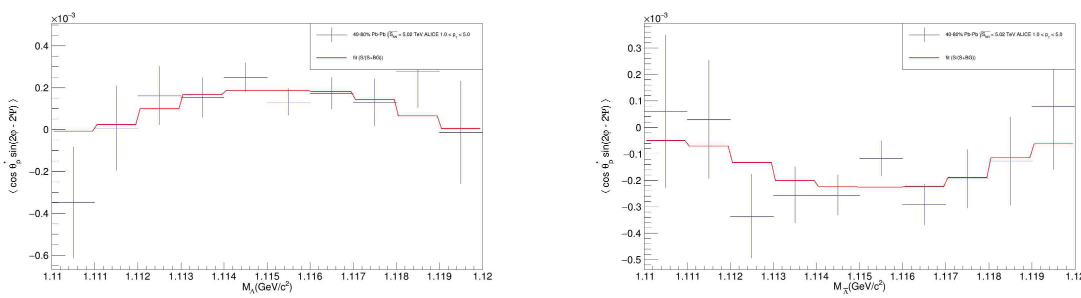

(a) (b)

Figure 6: Average cosine profile as a function of the invariant mass for **(a)** Λ and **(b)** $\bar{\Lambda}$, the red line shows the fitting using Eq.4.

In Fig.6 the $\bar{\Lambda}$ graph displays a concave shape, as opposite as the Λ one, this difference is due to the decay parameter but it's sign is accounted for and corrected in the polarization calculation.

In the second order, the polarization results as a function of centrality can be compared with those obtained from ALICE measurements.

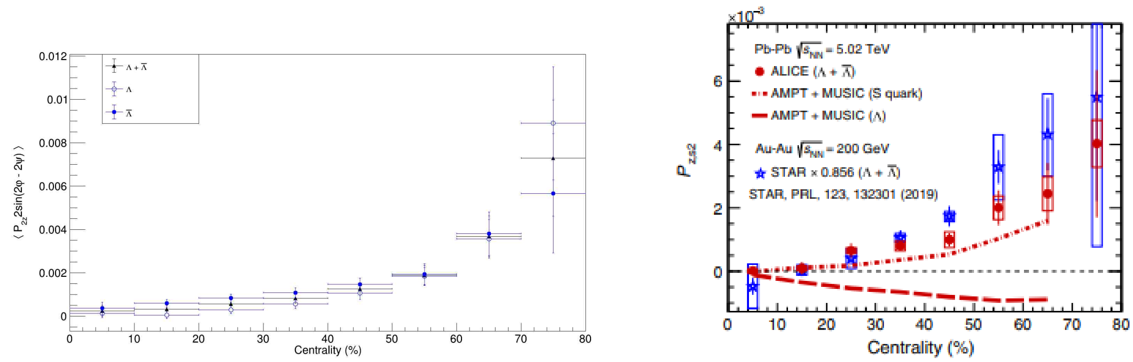

(a) (b)

Figure 7: **(a)** Measurements of second order polarization as a function of centrality for Λ,$\bar{\Lambda}$ and its average **(b)** Centrality dependence of $P_{z,s2}$ averaged for Λ and $\bar{\Lambda}$ in Pb-Pb collisions at $\sqrt{S_{NN}} =$ 5.36TeV and its comparison with the RHIC results for Au-Au collisions at $\sqrt{S_{NN}} = 200$GeV.

From Fig.7 it is possible to compare and conclude the expected increasing polarization pattern for the data analysis due to the elliptic flow as centrality increases. This effect is related to the dependence on the overlapping region and the initial shape of semi-peripheral collisions.

Another method for extracting the polarization signal involves using the observable Q foremen-tioned. By applying the invariant mass method to each bin interval from 1 to 6 (corresponding to $0 - 2\pi$), and subtracting this from the total polarization obtained from the entire interval, $P_{z,sn}$ can be computed. Fitting the results with Equation 1 yields the polarization value as the parameter asso-ciated with the sine function. This method is analogous to the previous one and should theoretically produce the same results. However, in this case, the results differed between the two analyses, likely due to variations in the constants used or other minor details that were not fully addressed. The two resulting graphs for both Λ and $\bar{\Lambda}$ showing the fitting of the data processed as mentioned above are shown in Fig.8.

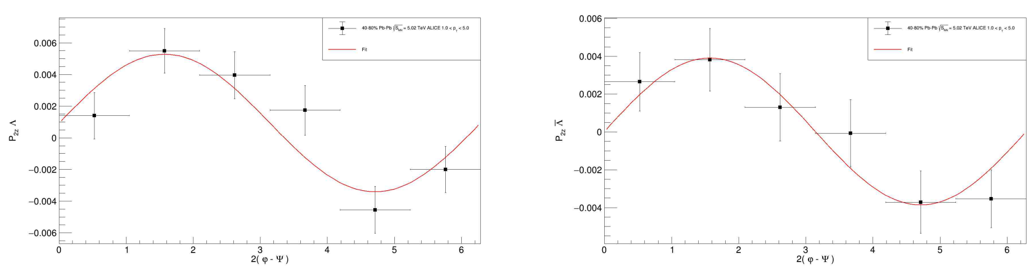

(a) (b)

Figure 8: Fitting of the computed by the invariant mass method polarization P_{2z} with the Equation 1 in second order event plane for **(a)**Λ and **(b)**$\bar{\Lambda}$.

5.3 Third Order Event Plane

The analysis procedure for the third order is essentially analogous to that of the second order, with replacing $n = 2$ for $n = 3$ in the equations and the use of the third-order dataset measurements. Fitting the profile using Equation 4 for the third order results in the graphs shown in Fig.9.

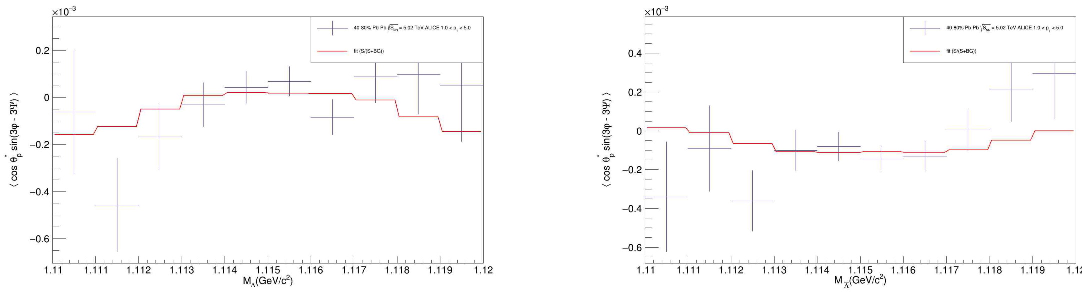

(a) (b)

Figure 9: Average cosine profile as a function of the invariant mass for **(a)** Λ and **(b)** $\bar{\Lambda}$, the red line shows the fitting using Eq.4.

The polarization obtained from the fitting is $P_z = 0.0036 \pm 0.0015$ for Λ and $P_z = 0.0043 \pm 0.0015$ for $\bar{\Lambda}$, consistent with the expected order of 10^{-3} for this effect. The behavior of the polarization can be analyzed as centrality increases, with an anticipated increase due to the geometry of the system. And, as shown in Fig.10, there is indeed an increase in polarization as centrality increases. Measurements of second order polarization as a function of centrality for Λ,$\bar{\Lambda}$ and its average

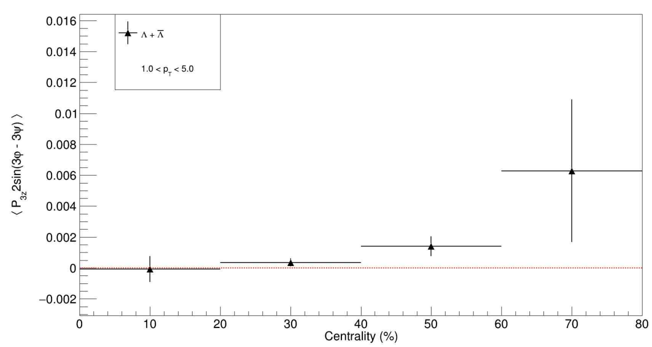

Figure 10: Average third-order polarization measurements for Λ and $\bar{\Lambda}$ as a function of centrality in the transverse momentum range $1.0 < p_T < 5.0$ GeV/c. Data obtained using the invariant mass method with reduced binning to increase statistics.

6 Conclusion

The goal of this analysis was to find evidence of the triangular flow hypothesis by measuring polarization in the third-order event plane. The Pythia simulation showed no signs of cosine modulation, which is expected since Pythia does not include second- or third-order flow in its simulations. This absence could lend credence to the hypothesis. By applying the methodology from the ALICE article [2], the results for second-order flow were verified and found to be consistent, showing a similar behavior of increasing with centrality. However, due to statistical uncertainties, no definitive conclusions could be taken. When applying the same method to the third-order, a hint of polarization and the expected dependence on centrality was observed. The results are not yet conclusive and measurements will be beneffited with data reconstruction and more event statistics in pass 4.

References

[1] M. I. Abdulhamid et al. "Hyperon Polarization along the Beam Direction Relative to the Second and Third Harmonic Event Planes in Isobar Collisions at $\sqrt{s_{NN}} = 200$ GeV". In: *Phys. Rev. Lett.* 131 (20 Nov. 2023), p. 202301. DOI: 10.1103/PhysRevLett.131.202301. URL: https://link.aps.org/doi/10.1103/PhysRevLett.131.202301.

[2] S. Acharya et al. "Polarization of Λ and $\overline{\Lambda}$ Hyperons along the Beam Direction in Pb-Pb Collisions at $\sqrt{s_{NN}} = 5.02$ TeV". In: *Phys. Rev. Lett.* 128 (17 Apr. 2022), p. 172005. DOI: 10.1103/PhysRevLett.128.172005. URL: https://link.aps.org/doi/10.1103/PhysRevLett.128.172005.

[3] T Scheib. "V 0 Reconstruction of Strange Hadrons in Au+Au Collisions at 1.23 AGeV with HADES". In: *Journal of Physics: Conference Series* 599 (Apr. 2015), p. 012030. DOI: 10.1088/1742-6596/599/1/012030.